1958ApJ...127..658A

# LINE BROADENING IN HIGH-LUMINOSITY STARS
## II. LESS LUMINOUS SUPERGIANTS*

HELMUT A. ABT
Yerkes and McDonald Observatories
*Received October 2, 1957; revised January 7, 1958*

ABSTRACT

Several types of line broadening are considered for I*b* supergiants Macroturbulence, in at least one likely form, gives profiles that are indistinguishable from rotational profiles. A magnetic field of 3800 gauss produces no broadening of λ 4508 Fe II but causes an apparent abundance increase of 38 per cent. Rotationally broadened profiles fit the observed ones and lead to a mean projected rotational velocity of 17 km/sec If conservation of angular momentum occurs, the rotational velocities are in accord with the evolution of I*b* supergiants from early B dwarfs, provided that supergiants do not rotate as rigid bodies The rotational-velocity distributions of the recovered and present B dwarfs agree in maximum, mean, and general form. On the other hand, if conservation of angular momentum does not occur due to mass loss, this mass would not be readily apparent. We are not able to choose between these two possibilities.

### I. INTRODUCTION

In Paper I (Abt 1957) it was shown that the profiles of lines in the spectra of A and F bright giants (luminosity class II) can be explained by using only the microturbulence (as determined from curves of growth) and rotation. Furthermore, if conservation of angular momentum can be assumed, then the rotational velocities are those to be expected from evolution of main-sequence stars via the Sandage-Schwarzschild tracks (1952) only if there is no radial transfer of angular momentum within the stars. Rigid-body rotation of bright giants, which would demand such a transfer, is incompatible with the small observed rotational velocities. These conclusions suffer because only ten stars were available for investigation.

In this paper the less luminous supergiants (luminosity class I*b*) are considered. Several types of line broadening are investigated, namely, macroturbulence (Sec. II), Zeeman splitting in a possible magnetic field (Sec. III), and rotation (Sec. IV). Our conclusions verify those summarized above for the bright giants.

The general technique involves computing profiles of λ 4508 Fe II for different types of motion and comparing these with observed profiles. The latter came from a homogeneous set of spectra of $8\frac{1}{2}$ A/mm dispersion of almost all the high-luminosity A and F stars brighter than $m_v = 8.0$.

### II. MACROTURBULENCE

The strengths of absorption lines lead to curves of growth which are characteristic of a mean Doppler velocity for each star. This velocity is identified as the mean random motion along the path of a single light-ray and is called the "microturbulent velocity." It is probably due to turbulence with eddy sizes not larger than the scale height of the atmosphere (about $10^6$ km for I*b* supergiants). Relative motions between various areas of the star's surface, such as in turbulent eddies and prominence-like activity appreciably larger in size than the scale height, will not affect the line strengths but will broaden the lines. We shall refer to this latter motion as "macroturbulence." Although microturbulence must be included when computing profiles of lines, we do not know beforehand whether any appreciable macroturbulence exists in I*b* supergiants.

The motion of prominences, for example, can be either vertical, horizontal, or a com-

* *Contributions from the McDonald Observatory,* No. 283.

bination of these. For simplicity of calculation, only vertical motion will be considered, and we shall assume a Gaussian distribution of upward and downward motion, i.e., a velocity function,

$$f(V, \mu) = \frac{1}{\sigma \mu (2\pi)^{1/2}} \exp\left[-\frac{1}{2}\left(\frac{V}{\sigma \mu}\right)^2\right], \tag{1}$$

where $V$ is the velocity; $\sigma$ is the dispersion; $\mu = \cos\theta$; and $\theta$ is the angular distance from the subsolar point.

The computed profile outside the spectrograph will be

$$R(\lambda - \lambda_0) = \int_0^1 d\mu \frac{I(0, \mu)}{I(0, 1)} \int_{-\infty}^{\infty} \frac{dV}{\sigma (2\pi)^{1/2}} e^{-1/2 V^2/(\sigma\mu)^2} R\left(\lambda - \lambda_0 - \frac{V}{c}\lambda_0, \mu\right) \div \int_0^1 d\mu\, \mu \frac{I(0, \mu)}{I(0, 1)}, \tag{2}$$

where $\lambda_0$ is the wave length at the center of the line and $I(0, \mu)/I(0, 1)$ is the monochromatic limb darkening. The profile $R(\lambda - \lambda_0 - V\lambda_0/c, \mu)$, as a function of position on the disk, is Chandrasekhar's exact solution (1950) to the equation of transfer and involves the microturbulent velocity. The computed profile, instrumentally broadened, is then the solution of

$$R_{\text{comp}}(\lambda - \lambda_0) = \int_{-\infty}^{\infty} I(\lambda - \lambda') R(\lambda' - \lambda_0)\, d\lambda', \tag{3}$$

where $R(\lambda' - \lambda_0)$ is the result of equation (2) and $I(\lambda - \lambda')$ is the instrumental profile

Equations (2) and (3) have been solved numerically for a number of velocity dispersions and line strengths, in order to match the observed profile of λ 4508 Fe II in α Persei. The best agreement (Fig. 1) occurs for a dispersion of 13 km/sec. For comparison, the profile for a rotational velocity of 20 km/sec is shown. The observations are not accurate enough to distinguish which type of broadening exists in this star, particularly if there is a mixture of both.

In Section IV the observed profiles in other supergiants will be compared with rotationally broadened profiles, but as good agreement could be obtained with a random vertical motion where $\sigma = \frac{2}{3} V_{\text{rot}} \sin i$. However, evolution from the rapidly rotating main-sequence B stars requires that supergiants have a certain amount of line broadening due to rotation; if no more than this amount is required to explain the observed profiles, then we shall conclude that macroturbulence does not exist to any appreciable extent.

## III. ZEEMAN BROADENING

No definite reports have been published of magnetic fields in supergiants. This is due, in part, to the large breadth of their lines. However, we may inquire about the effect on line profiles of a moderate magnetic field.

Specifically, we shall consider the profile in integrated light of λ 4508 Fe II in an F5 I*b* star having (1) a microturbulence of 6.4 km/sec, which is typical for this class (see Table 1); (2) a rotational velocity of 20 km/sec; and (3) a dipole field with a strength of 5000 gauss at the poles. It will be assumed that the rotational and dipole axes coincide and are perpendicular to the line of sight. The difficult problems connected with absorption and re-emission of polarized radiation in a stellar atmosphere will be ignored by treating all components as unpolarized. Therefore, the results are approximate.

The predicted Zeeman pattern for this line is shown in Figure 2. The separations of the components are shown in fractions of the normal Zeeman triplet spacing. However, the scale in angstroms depends on position on the disk, since the magnetic-field strength is

$$H(\mu) = \frac{1}{2} H_p (1 + 3\mu^2)^{1/2} , \tag{4}$$

where $H_p$ is the polar field strength and $\mu = \cos\theta$. The computed relative intensities are independent of the type of coupling involved, but the relative amounts of $p$ and $s$ components observed at each position ($\theta$, $\phi$) on the disk will depend on the direction of $H$ at that point relative to the direction of the line of sight.

The profile should be computed as follows: For each of a large number of elements of area on the disk, compute the Zeeman pattern, add the line-absorption coefficient profiles for the various components, and compute the residual absorption profile from the solution to the equation of transfer. Then shift the profile in wave length by an amount depending on the projection of the rotational velocity on the line of sight, multi-

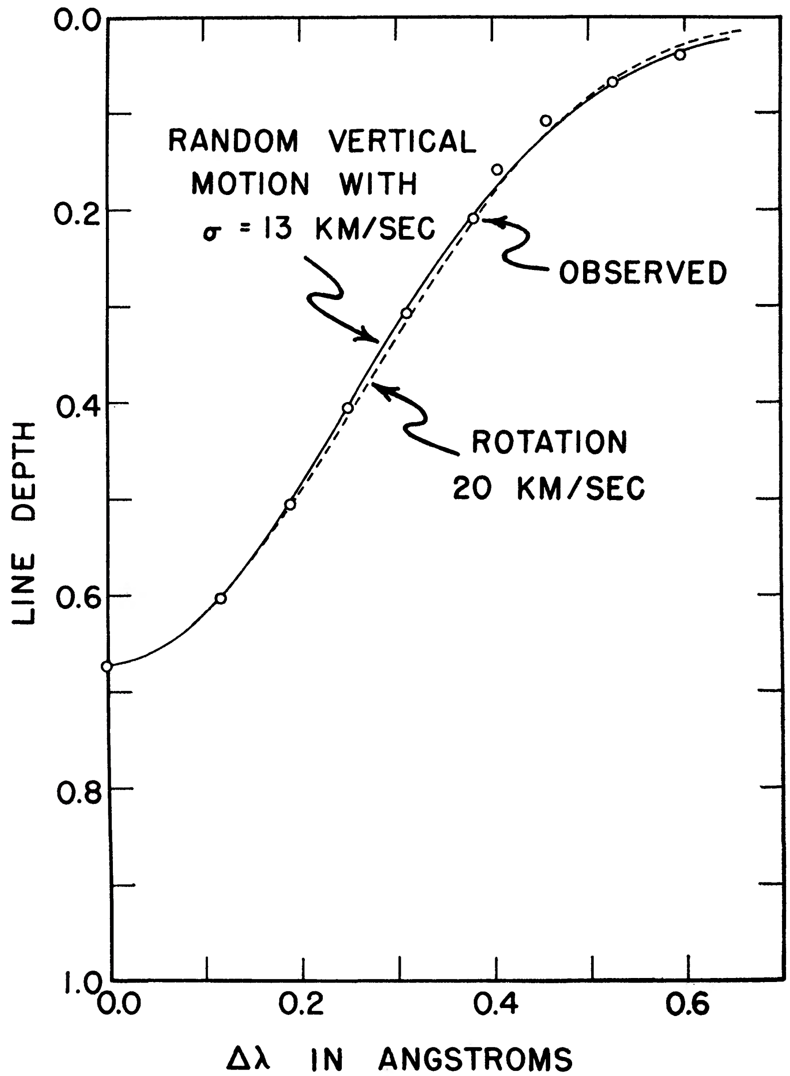


FIG. 1.—The measured profile (*circles*) of λ 4508 Fe II in α Persei and two computed profiles. The solid curve was computed for macroturbulence with a Gaussian distribution of vertical motions, and the dashed curve is for rotation Both include a microturbulent velocity of 6.4 km/sec.

ply by the limb-darkening ratio and the projected area, and add the contributions from the various elements of area. This involves a prohibitive amount of computation. However, it was found that the relative intensities in the Zeeman pattern and the field strength varied by an average of only 11 and 20 per cent, respectively, about their mean values. So it was assumed that the Zeeman pattern in integrated light is constant over the disk and is characteristic of a field of 3800 gauss.

The resultant profile is indistinguishable (i.e., a mean difference of 0.13 per cent) from a profile computed for no magnetic field but with an abundance increased by a factor of 1.38. Thus a moderate magnetic field of 3800 gauss produces no broadening

TABLE 1

PHYSICAL PARAMETERS FROM CURVES OF GROWTH

| | STAR | | | | | | |
|---|---|---|---|---|---|---|---|
| | HR 8345 | HR 2874 | α Lep | ν Aql | α Per* | 35 Cyg | HR 690 |
| Spectrum | A2 I*b* | A5 I*b* | F0 I*b* | F2 I*b* | F5 I*b* | F5 I*b* | F7 I*b* |
| log $a$ | <−1 8 | −1 8 | −3 0 | −2 8 | −2 7 | −3 0 | −3 0 |
| $v$ (km/sec) | 7.5 | 5.2 | 6.9 | 7 2 | 6.3 | 6.5 | 6.3 |
| $T_{\text{ion}}$ | 10290 | 7000 | 6550 | 6460 | 6150 | 5730 | 5600 |
| log $P_e$ | +1 55 | +0 12 | +0 03 | +0 16 | +0.1 | −0 48 | −0 65 |

* Data taken from Greenstein (1948)

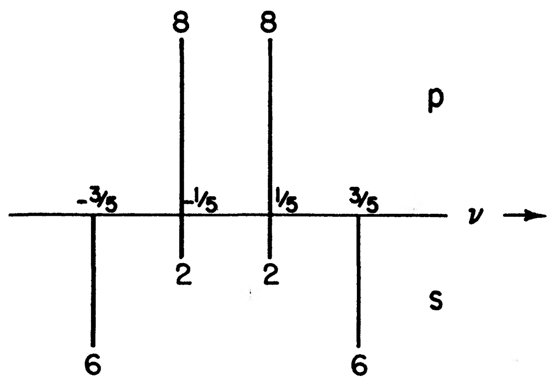


FIG. 2.—The Zeeman pattern for λ 4508 Fe II The relative intensities, represented by the integers and vertical extent of the lines, are on an arbitrary scale The splitting in frequency is in fractions of the normal Zeeman triplet spacing.

of this line but rather a magnetic intensification (Babcock 1949) of 38 per cent. This line is on the horizontal section of the curve of growth where the largest intensification is to be expected, but it has a fairly narrow Zeeman pattern

## IV. ROTATION

The parameters from curves of growth for a sample of I*b* supergiants are given in Table 1. These were obtained from line intensities measured on the same spectrograms as those used for the profiles and by a method described in Paper I. The variation in these parameters with spectral type and luminosity will be discussed in a later paper; for the present we are concerned primarily with the Doppler velocity, $v$, which is nearly identical with the microturbulent velocity. It was determined with an accuracy of $\pm 0.5$ km/sec. The profiles are very insensitive to the amount of limb darkening, and the shapes (but not the strengths) are insensitive to temperature. The spectral types in Tables 1 and 3 are by either Johnson and Morgan (1953) or Bidelman (1951).

The measured profiles are given in Table 2. They include an instrumental broadening, as determined from the comparison lines, which can be described by the Voigt parameters (van de Hulst and Reesinck 1947), $h = 0.226$ A and $\beta_1/\beta_2 = 0.59$.

The method of computation was described in Paper I. Profiles were computed for four groups of stars, namely, A0–A2, A3–A5, F0–F3, and F5–F8. We assumed $v = 6.4$ km/sec for each group except F0–F3; both members of this group are in Table 1 and have an average Doppler velocity of 7.0 km/sec. For other parameters we used means of data in Table 1, plus the assumption of pure scattering. Profiles were computed for a variety of line strengths in each group and for rotational velocities in steps of 10 km/sec.

The computed profiles fit the measured ones rather well, but slightly less accurately than in the case of the bright giants (see Fig. 2 of Paper I). The mean differences, measured *minus* computed, were 0.90 and 0.61 per cent for the class I*b* and II stars, respectively. These are well within the expected errors for photographic photometry. The accuracy in $V \sin i$ is estimated to be $\pm 3$ km/sec for each star. The fourth and fifth columns of Table 3 give the rotational velocities as determined here and by Herbig and Spalding (1955). We again conclude that the estimates by the latter authors are very reliable.

Included in Table 3 are two stars of intermediate luminosity class, I*b*–II. For these stars the measured profiles were compared with ones computed for I*b* stars rather than class II, since the measured profiles are more characteristic of the higher microturbulent velocity. Not included in the list is the peculiar (Bidelman 1951) high-latitude supergiant HD 161796, whose line profiles also appear to be peculiar.

The rotational velocities range from 10 to 28 km/sec. The distribution is slightly peculiar in the lack of velocities less than 10 km/sec. The same thing is true for the bright giants. Out of twenty-five stars, one would expect to find four or five in this range. This deficiency may be an indication that the rotational velocities were systematically overestimated by an additive constant, such as would be due to a small amount of macroturbulence.

We can derive the rotational velocities of the main-sequence stars from which these supergiants evolved and make a comparison with present main-sequence stars if we assume that angular momentum is conserved during evolution. However, it is not obvious that this quantity should be conserved. Therefore, we shall distinguish between two possibilities: in Section V we consider the consequences of assuming conservation of angular momentum, while in Section VI we consider the possibility that angular momentum has been lost. We find that we shall not be able to choose between these two alternatives on the basis of the present material.

## V. CONSERVATION OF ANGULAR MOMENTUM

Assuming the Sandage-Schwarzschild (1952) evolutionary tracks and conservation of angular momentum for each star as a whole, we can compute the rotational velocities of these stars when they were on the main sequence, provided that we know the amount of redistribution of angular momentum within the stars. Following Oke and Greenstein (1954), we again consider two extremes: (A) rigid-body rotation, which involves a radial transfer of angular momentum within the stars, and (B) differential rotation, involving no radial transfer of angular momentum. Oke and Greenstein's computations of the changes in moment of inertia in the Sandage-Schwarzschild models were used for case A; for case B the velocity decrease is simply proportional to the radius increase, $R/R_0$, given in the third column of Table 3. Initially, A and F I*b* supergiants were at about B2.5 V. We assumed $M_v = -4.5$ for all I*b* stars (Keenan and Morgan 1951).

TABLE 2

OBSERVED LINE PROFILES, $R(\lambda - \lambda_0)$

| $\lambda-\lambda_0$ (A) | STAR | | | | | | | | | | | | | | |
|---|---|---|---|---|---|---|---|---|---|---|---|---|---|---|---|
| | 13 Mon | η Leo | HR 8345 | HR 8443 | HR 2874 | α Lep | ν Aql | α Per | HD 172052 | 35 Cyg | HR 690 | 45 Dra | γ Cyg | HR 7055 | HR 7542 |
| 0.00 | 0 400 | 0.480 | 0.513 | 0.540 | 0.610 | 0.698 | 0.745 | 0.673 | 0.710 | 0.765 | 0.785 | 0.770 | 0.820 | 0.680 | 0.585 |
| .05 | .386 | 470 | .500 | .526 | .586 | 679 | .724 | 657 | .685 | 748 | 771 | 752 | .801 | 665 | .578 |
| .10 | .353 | 439 | 468 | 498 | .540 | 630 | 666 | 622 | .634 | 694 | 731 | 715 | 767 | 627 | .556 |
| .15 | .298 | .385 | 412 | 455 | 469 | .550 | .585 | .564 | .560 | 614 | .660 | 655 | 714 | .557 | .519 |
| .20 | .234 | .318 | .350 | 403 | .385 | 455 | 493 | 490 | 455 | .516 | .561 | .579 | 641 | 465 | 470 |
| .25 | .169 | .250 | .285 | .346 | .309 | .381 | .397 | 407 | .332 | 402 | 443 | 480 | .546 | .363 | 413 |
| .30 | .114 | .188 | .221 | .288 | .240 | .261 | .294 | .324 | .224 | .290 | .323 | .370 | 430 | .272 | .352 |
| .35 | 070 | .135 | .163 | .233 | 182 | .183 | .203 | .245 | .146 | .196 | .210 | .266 | .319 | .194 | .285 |
| .40 | 0.040 | 087 | .115 | .182 | .134 | .125 | .131 | .170 | 090 | 120 | .124 | .183 | .215 | .132 | .223 |
| .45 | | 053 | 078 | 135 | 095 | 080 | 077 | .115 | 053 | 073 | .070 | .119 | .134 | 087 | .169 |
| .50 | | 0.031 | 049 | 092 | 065 | 0.049 | 0.046 | 078 | 0 033 | 0 044 | 0.037 | 077 | 085 | 054 | 122 |
| .55 | | | 0.030 | 055 | 0.045 | | | 050 | | | | 0 047 | 052 | 0 034 | 085 |
| .60 | | | | 0 031 | | | | 0 031 | | | | | 0 030 | | 057 |
| 0.65 | | | | | | | | | | | | | | | 0 037 |

The initial rotational velocities for these two cases are given in the last two columns of Table 2. The means are 77 and 177 km/sec for cases A and B, respectively. These should be compared directly with Slettebak and Howard's (1955) mean rotational velocity of 158 km/sec for B2–B5 V stars. The rotational velocities determined here for I*b* supergiants are too small by a factor of 2 to be compatible with rigid-body rotation. This is the same conclusion as that reached for the bright giants; it is now based on a total of twenty-five stars. For case B the rotational velocities determined here are 12 per cent too high. If this difference is significant, it may be due either to a small transfer of angular momentum from the central region of the stars to the surface layers or to an overestimate of the rotational velocities due to a small amount (not more than 2 km/sec) of macroturbulence. The evolutionary tracks are unlikely to be incorrect by the 3 mag. which would be required to force agreement with rigid-body rotation.

TABLE 3

ROTATIONAL VELOCITIES OF I*b* SUPERGIANTS

| STAR | SPECTRUM | $R/R_0$ | $V$ SIN $i$ (km/sec) | | | |
|---|---|---|---|---|---|---|
| | | | Present (Abt) | Present (Herbig and Spalding) | Initial (A) | Initial (B) |
| 13Mon | A0 I*b* | 6 0 | 15 | | 43 | 90 |
| $\eta$ Leo | A0 I*b* | 6 0 | 20 | | 57 | 120 |
| HR 8345 | A2 I*b* | 6 5 | 21 | . | 65 | 137 |
| HR 8443 | A3 I*b* | 7 0 | 26 | | 85 | 182 |
| HR 2874 | A5 I*b* | 7 5 | 20: | . . | 69 | 150 |
| $\alpha$ Lep | F0 I*b* | 8 9 | 15 | 15 | 61 | 134 |
| $\nu$ Aql | F2 I*b* | 10 0 | 13 | <20 | 61 | 130 |
| $\alpha$ Per | F5 I*b* | 13 2 | 20 | 20 | 113 | 265 |
| HD 172052 | F5 I*b* | 13 2 | 12 | . . | 68 | 159 |
| 35 Cyg | F5 I*b* | 13 2 | 13 | <15 | 73 | 172 |
| HR 690 | F7 I*b* | 17 4 | 10: | . | 75 | 174 |
| 45 Dra | F7 I*b* | 17 4 | 17 | <20 | 128 | 296 |
| $\gamma$ Cyg | F8 I*b* | 19 5 | 15: | <15 | 112 | 293 |
| Mean | | | 17 | | 77 | 177 |
| HR 7055 | F2 I*b*–II | 6 7 | 16 | | 50 | 107 |
| HR 7542 | F8 I*b*–II | 12 7 | 28 | | 170 | 354 |

The differential rotation is in the sense that the interior is rotating with a larger angular velocity than the surface region. We may ask whether it is possible for a star to rotate in this manner, since a magnetic field of only a few gauss is required to prevent differential rotation. This objection can be overcome if the shape of the field is such as not to bind the inner and outer layers, e.g., a toroidal field.

A total of twenty-five stars is perhaps sufficient to consider the frequency distribution in $V$ sin $i$. Figure 3 shows this distribution for the initial dwarfs, compared to present dwarfs according to Slettebak and Howard. Both distributions have a maximum between 100 and 200 km/sec, terminate at 400 km/sec, and have approximately the same mean value; they are sufficiently similar to lend support to the interpretation of line broadening in bright giants and I*b* supergiants as due to microturbulence and rotation.

This conclusion that A and F bright giants and I*b* supergiants do not rotate as rigid bodies would seem to be contradictory to Sandage's (1955) conclusions based on Slettebak's rotational velocities. Sandage found numerous stars which rotate too rapidly to be compatible with differential rotation and the observed maximum of 400 km/sec for present main-sequence stars. However, all his stars for which differential motion cannot apply are ones which have increased their radii by not more than a factor of 4. Among Sandage's stars (in the complete range from B0 to G0) with expansions by more than 4, there are no cases of rotation too rapid for differential rotation to occur. All twenty-five of the stars in the present consideration also have expanded by more than a factor of 4. Therefore, we suggest that during the initial expansion (to a factor of about 4) a star continues to rotate as a rigid body but that subsequently it commences to rotate differentially.

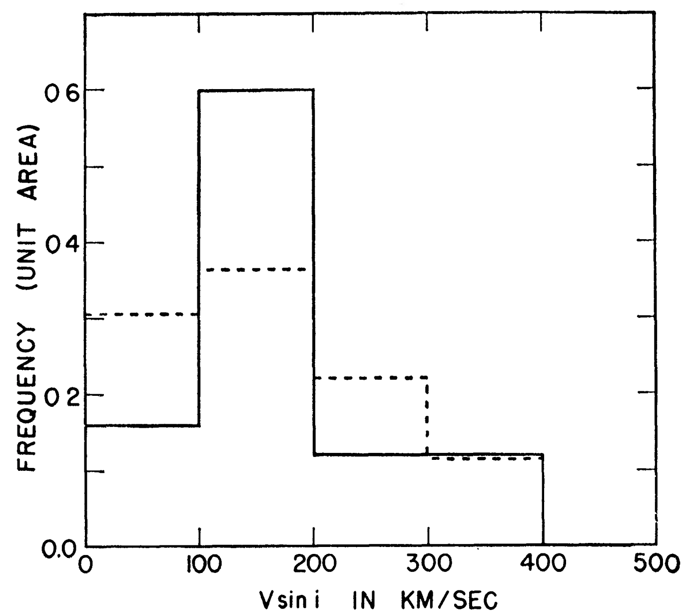


FIG. 3 —The relative frequencies of various projected rotational velocities for seventy-eight B2–B5 V stars (*dashed line*) according to Slettebak and Howard, and for the initial dwarfs of twenty-five present supergiants and bright giants (*solid line*).

## VI. NON-CONSERVATION OF ANGULAR MOMENTUM

Let us reverse the previous argument by assuming that both dwarfs and supergiants rotate as rigid bodies. Then, from the discrepancy between $\langle V \sin i \rangle$ (initial) = 77 km/sec (Table 3, case A) and $\langle V \sin i \rangle$ (B2–B5 V) = 158 km/sec (Slettebak and Howard 1955), we conclude that the supergiants have lost half their angular momentum. This could come about in two ways: either by interaction of the star's magnetic field with an interstellar magnetic field or by mass loss. The first of these is hypothetical because it is not known whether these stars have significant magnetic fields and the effect is difficult to evaluate without a specific model, but the second can be treated.

Assume that a normal dwarf with a Cowling model interior loses angular momentum by losing an exterior layer of material. Then, to lose half of its angular momentum, this rigid body must lose 22 per cent of its mass. If this occurs at a uniform rate during its evolution from the zero-age main sequence, namely, $4 \times 10^7$ years for I*b* supergiants, the rate of mass loss is $3 \times 10^{18}$ gm/sec. Assume that the material leaves the surface at the velocity of escape. Then, under equilibrium conditions, each radial column 1 $cm^2$ in cross-section will contain 0.003 gm. This material will not be detectable in the continuum but may be apparent at Hα, particularly if the mass loss is not at a uniform rate or if we consider more luminous stars whose velocities of escape are smaller. We conclude that a loss of angular momentum by mass loss is a possibility.

If mass loss does occur, we cannot, with the present material, specify what fraction of the mass and angular momentum has been lost. Therefore, we are unable to describe the type of rotation (rigid-body or differential) or how much macroturbulence (if any) is present. Since we derived only maximum rotational velocities, we obtain only minimum mass losses. We are unable to choose between differential rotation and mass loss with the present material, but one or both of these effects very likely occur.

Part of the calculations were made by Mr. James R. Burd. The author is indebted to Dr. Leon Mestel and to several members of the Yerkes staff for profitable conversations.

## REFERENCES

Abt, H. A. 1957, *Ap. J.*, **126**, 503.
Babcock, H. W. 1949, *Ap. J.*, **110**, 126.
Bidelman, W. P. 1951, *Ap. J.*, **113**, 304.
Chandrasekhar, S. 1950, *Radiative Transfer* (Oxford: Clarendon Piess), p 327.
Greenstein, J. L. 1948, *Ap. J.*, **107**, 151.
Herbig, G. H., and Spalding, J. F., Jr. 1955, *Ap. J.*, **121**, 118.
Hulst, H. C. van de, and Reesinck, J. J. M. 1947, *Ap. J.*, **106**, 121.
Johnson, H. L., and Morgan, W. W. 1953, *Ap. J.*, **117**, 313.
Keenan, P. C., and Morgan, W. W. 1951, *Astrophysics*, ed J. A. Hynek (New York: McGraw-Hill Book Co.), p. 23.
Oke, J. B. and Greenstein, J. L. 1954, *Ap. J.*, **120**, 384.
Sandage, A. R. 1955, *Ap. J.*, **122**, 263.
Sandage, A. R., and Schwarzschild, M. 1952, *Ap. J.*, **116**, 463
Slettebak, A., and Howard, R. F. 1955, *Ap J.*, **121**, 102.